Investigation of undercooled liquid metals using XAFS, temperature scans and diffraction

Adriano Filipponi,[a]* Andrea Di Cicco,[b] Simone De Panfilis,[b] Angela Trapananti,[b] Jean-Paul Itiè,[c] Michael Borowski[d] and Stuart Ansell[d]

[a]Istituto Nazionale di Fisica della Materia and Dipartimento di Fisica, Università dell' Aquila Via Vetoio, 67010 Coppito, L' Aquila, Italy, [b]Istituto Nazionale di Fisica della Materia and Dipartimento di Matematica e Fisica, Università di Camerino, Via Madonna delle Carceri, 62032 Camerino (MC), Italy, [c]LPMC, Université Paris 6, 2 place Jussieu, F-75005 Paris, France, and [d]European Synchrotron Radiation Facility, BP 220, F-38043 Grenoble, France. E-mail: adriano.filipponi@aquila.infn.it

Novel techniques and the experimental station for experiments on condensed matter under extreme conditions that have been developed at the BM29 beamline of the European Synchrotron Radiation Facility (ESRF) are described. The experimental setup includes facilities to collect high-quality extended X-ray absorption fine structure (EXAFS) spectra, to perform controlled temperature scans while monitoring the sample absorption for the direct detection of phase transitions, and to collect high-resolution energy-scanning X-ray diffraction (ESXD) data, with recent enhancements through the installation of a two-channel collimator detector system. Facilities for X-ray absorption temperature scans, introduced five years ago, are now exploited for a wide variety of purposes. A method for the measurement of the nucleation rate in undercooled liquids has been proposed recently. All these advances in the experimental setup and techniques, combined with a simple but rigorous X-ray absorption fine structure (XAFS) data analysis scheme for disordered matter, have contributed to make feasible challenging experiments on undercooled liquid matter that were not even conceivable only a few years ago. An example of the application of these methods to undercooled liquid indium (In) is presented.

Keywords: undercooled liquid indium; temperature scans; condensed matter.

1. Introduction

X-ray absorption spectroscopy (XAS) has a great potential to provide a physical insight into condensed matter in the liquid state, especially in investigations under non-standard sample conditions of high pressure and/or high temperature. A large number of challenging experiments have been performed in recent times by various groups (Hosokawa *et al.*, 1992; Tamura *et al.*, 1995; Filipponi *et al.*, 1997; Wallen *et al.*, 1998; Buontempo, Filipponi, Postorino & Zaccari, 1998; Katayama *et al.*, 1999) adopting a variety of experimental techniques and obtaining very interesting and unique results. A review article has been published recently on this subject (Filipponi, 2001).

The undercooled state of liquid matter is rather elusive and for the same reason quite interesting. In the absence of external driving forces, such as the presence of a crystalline seed, liquid substances can be usually undercooled well below the respective melting temperatures T_m. The explanation of such apparently mysterious behaviour is given by simple thermodynamical considerations, first formulated by Turnbull (1950) within the framework of the so-called classical theory of nucleation. A thermodynamical system, initially in the liquid state, can only be driven to the stable crystalline phase by spontaneous fluctuations in the configurational space, leading to the formation of a crystalline nucleus. In order for the system to crystallize, the nucleus has to grow above a critical size which corresponds to a maximum of the Gibbs free energy. The change in the free energy associated with the formation of a nucleus of size n can be expressed as (Turnbull, 1950)

$$\Delta G(n) = n\Delta G_v + n^{2/3}\Delta G_s, \tag{1}$$

where the first volume term $\Delta G_v \simeq -a(T_m - T)$ is negative below T_m, while the second surface term ΔG_s is positive and accounts for the interfacial energy. For small n, the latter term dominates and the function exhibits a maximum for $n = n^* \propto (T_m - T)^{-3}$, the value of which is $\Delta G^* \propto (T_m - T)^{-2}$. The divergent behaviour of the critical size nucleus and of the free-energy barrier explain why spontaneous crystallization does not occur for T close to T_m. The overall probability of the nucleation path is dominated by the probability of overcoming the barrier (Turnbull, 1950) and therefore can be expressed by an Arrenius functional form of the type

$$\begin{aligned} I(T) &\simeq A\exp(-\Delta G^*/k_B T) \\ &= A\exp[-b/T(T_m - T)^2]. \end{aligned} \tag{2}$$

This expression defines the rate of nucleation $I(T)$ of an undercooled liquid into the stable crystalline solid. This fundamental physical quantity measures the formation rate of critical nuclei per unit volume in the melt. When a nucleus is formed, the spontaneous crystallization cannot be stopped and all the sample crystallizes.

Efforts to perform physical measurements in the undercooled liquid state involve a competition against the tendency of the sample to crystallize. This can be achieved by operation under high-purity conditions or/and by exploiting the dependence on the sample size. A research effort on the extended X-ray absorption fine structure (EXAFS) of undercooled liquid alloys has been carried out by Egry and co-workers by using the electromagnetic levitation technique (Jacobs *et al.*, 1996; Jacobs & Egry, 1999). In these experiments, the containerless environment enables operation under high-purity conditions and attainment of deep undercooling on samples of size of the order of millimetres. An alternative way to achieve deep undercooling consists of working with particles of micrometre size, thus gaining a factor of the order of 10^9 in the particle volume, corresponding usually to several tens of degrees in temperature. Experiments have been performed on Hg and Ga emulsions (Ottaviano *et al.*, 1994; Di Cicco, 1998) and powder mixtures of Ge/BN (Filipponi & Di Cicco, 1995), Rh/HfO_2 (Di Cicco *et al.*, 1999) and Pd/Al_2O_3 (Filipponi *et al.*, 1999). With these techniques, in spite of the intrinsic low-purity conditions, undercooling of a few 100 K could be reached, especially in Ge and Pd. In the course of our long-term research project, we realised that upgrades of the standard experimental stations for X-ray absorption spectroscopy and the development of complementary techniques to probe other sample properties were highly advisable. At the same time, improvements of the XAFS data analysis techniques for liquids were also needed. The major advances achieved by our group in these fields will be illustrated in the following sections, including some recent unpublished material.

2. Advances in the experimental methods

Experimental work was initially performed at Frascati, and at the D42 and D44 beamlines at Orsay (LURE) (Ottaviano *et al.*, 1994;

Filipponi & Di Cicco, 1995). After 1995, all efforts were concentrated on the realisation of an advanced experimental station at the BM29 beamline of the ESRF (Filipponi *et al.*, 1998; Filipponi, Borowski *et al.*, 2000; Filipponi, Di Cicco *et al.*, 2000). Two sample-environment chambers to generate high-temperature and high-pressure conditions were developed. In particular, a high-temperature oven has been designed and built for the LURE facility (Filipponi & Di Cicco, 1994) and has been widely exploited and improved at later stages (Filipponi *et al.*, 1998; Filipponi, Borowski *et al.*, 2000; Filipponi, Di Cicco *et al.*, 2000). This system turned out to be extremely versatile, simple to use and of good performance. The other experimental technique that has been exploited is the high-pressure–high-temperature (HP–HT) technique based on the use of the Paris–Edinburgh press originally developed at LURE by the Paris group (Besson *et al.*, 1992; Katayama *et al.*, 1997). Our attempt to develop an ideal and versatile setup for XAFS experiments under extreme conditions and the major developments at the BM29 experimental station are described in detail elsewhere (Filipponi, Borowski *et al.*, 2000; Filipponi, Di Cicco *et al.*, 2000). A simplified scheme of the experimental setup is presented in Fig. 1, where the system of three ionization chambers for the simultaneous X-ray absorption measurements of a sample and a reference sample is clearly indicated. In addition, Fig. 1 shows a schematic drawing of the temperature control system for a typical oven setup and a sketch of a two-channel collimator/detector system to record X-ray diffraction. This system is a new development and is described in detail in the next subsection.

2.1. *Energy-scanning X-ray diffraction*

Scientists familiar with XAFS will be aware of the limited sensitivity of the technique to crystalline ordering and to the presence of impurities in the sample. More specifically, in the investigation of undercooled liquids with the droplet technique, by which the nucleation of the droplets is independent and which leads to no qualitative difference between the XAFS spectra of a hot solid or a liquid, from the basis of XAFS alone it is not possible to identify whether or not part of the sample has crystallized. Similarly, the possibility of small sample contamination, especially at high temperature, is not remote. In a careful experiment, every effort should be made to exclude or control the possibility that the sample transforms (even partly) into some unwanted form. Chemical or X-ray analysis after the experiment is often not sufficient to identify all possible problems; for instance, certain types of contamination can be reversible (*i.e.* occur only at high T) and can hardly be identified after the experiment. A very effective solution to this problem is offered by the possibility to implement an efficient *in situ* X-ray diffraction detection system on standard XAFS setups. Setups combining, in various ways, XAFS and X-ray diffraction (XRD) have indeed been developed (Clausen, 1998; Dent *et al.*, 1992; Sankar *et al.*, 1993), mainly in the context of advanced chemical research.

The technique we have proposed (Filipponi, Borowski *et al.*, 2000; Filipponi, Di Cicco *et al.*, 2000) consists of the installation of a two-slit collimator, collecting the diffracted radiation either in the vertical or in the horizontal plane. The collimator is fixed and the diffraction scan is performed by scanning the monochromator energy. This technique, referred to as energy-scanning X-ray diffraction (Filipponi, Borowski *et al.*, 2000; Filipponi, Di Cicco *et al.*, 2000), turned out to be much simpler than the possible alternative installation of an angular scanning X-ray diffraction system around the sample, and provides much better performance in terms of resolution with respect to the use of a position sensitive detector or when compared with the performance of a typical energy dispersive X-ray diffraction detection system (which requires in any case a white beam).

The characteristics of this diffraction detection system are rather encouraging. Alignment takes usually less than 1 h and is performed on a Bragg peak of the sample powder or of other crystalline compounds pelleted with the sample (matrix, calibrants). The energy position of the Bragg peak allows the angle to be determined precisely. The system will remain fixed during the entire experiment and the only additional alignment will be required at sample changes when the sample will have to be aligned in the centre of the scattering volume defined by the X-ray beam and the collimator acceptance path.

This system guarantees an excellent resolution and a high reproducibility of the powder diffraction scans. The width of the Bragg peaks on the energy scale is of the order of 10^{-3} of the peak energy, which guarantees a sensitivity in lattice-spacing determinations of the order of one part in 10^4 or better.

This system has been used for various purposes. In an experiment on undercooled liquid Pd (Filipponi *et al.*, 1999), it has been checked that the Pd Bragg peaks were absent after the XAFS measurements in the undercooled liquid state. Additional results on the Pd and Pd/C systems and, in particular, on the precise determination of the lattice-spacing expansion as a function of temperature were published separately (Filipponi, Borowski *et al.*, 2000; Filipponi, Di Cicco *et al.*, 2000). The system has also been widely applied in high-pressure experiments in order to determine the sample pressure through the measurement of the lattice spacing of a calibrant compound with known equation of state (Buontempo, Filipponi, Martínez-García *et al.*, 1998).

The q range accessible with ESXD depends on the collimator angle and energy range of the scans according to $q = 4\pi \sin(\theta)/c/hE$. The efficiency of the collection can be largely improved by adopting a multichannel detector system in which the various collimators are

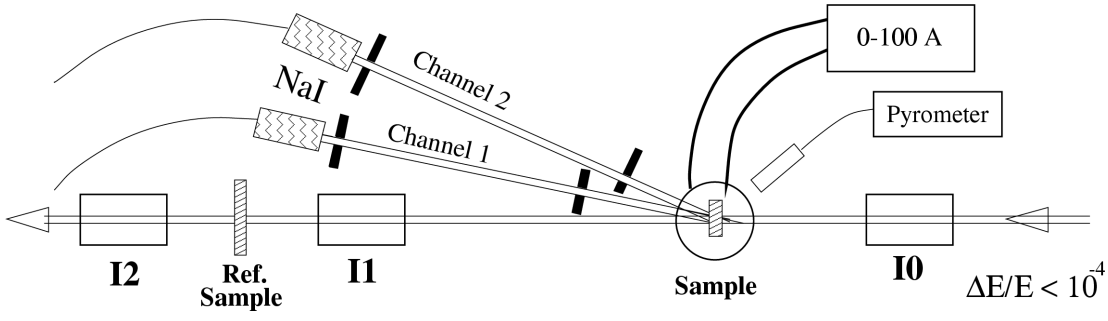

Figure 1
Details of the ESRF BM29 experimental station, downstream the monochromator. In this setup, monochromator energy scans can be used to record either X-ray absorption spectra or the powder diffraction pattern collected in the two fixed-angle high-resolution collimator detector channels. In addition, the remotely piloted high-current power supply and the temperature probe (pyrometer) can be used to scan the sample temperature.

placed at several angles in the range 2θ = 10–40°. In such a case, a broader q range can be probed by overlapping scans collected simultaneously by the various detectors in narrower energy ranges. The principle of operation of a multichannel detector has been tested with the two-channel setup of Fig. 1, as described in §5.

2.2. *X-ray absorption temperature scans*

Another experimental technique that we have developed at BM29 is based on the monitoring of the sample absorption at one or more energy points of interest during controlled scans of the sample temperature (Filipponi, 1996; Filipponi *et al.*, 1998; Filipponi, Borowski *et al.*, 2000; Filipponi, Di Cicco *et al.*, 2000). This scanning mode turned out to be a very powerful tool for sample diagnostics and to perform various physical measurements.

The principle of the method is based on the occurrence of discontinuous changes of the shape of X-ray absorption spectra at first-order phase transitions. By monitoring the sample absorption at an energy corresponding to a point of high sensitivity, as a function of the sample temperature, the phase transition can be revealed with an excellent temperature resolution. Examples of phase transitions studied with this technique include solid-solid phase transitions and melting. The presence of a hysteresis can be easily detected. Applications of this technique to the melting and undercooling of elemental liquids were extremely successful (Filipponi *et al.*, 1998, 1999; Filipponi, 1996).

The technique is useful for a wide range of applications, such as: (i) detection of solid–solid phase transitions (Filipponi *et al.*, 1998); (ii) detection of melting and undercooling (Filipponi *et al.*, 1998, 1999); (iii) checking the calibration of a temperature probe; (iv) preparation of the sample in a well defined phase (including metastable states) prior to an EXAFS measurement (Filipponi *et al.*, 1999); (v) determination of the liquidus curve of simple binary eutectic alloy with a single measurement (Filipponi *et al.*, 1998); (vi) determination of the eutectic temperature of an alloy (Filipponi, Borowski *et al.*, 2000; Filipponi, Di Cicco *et al.*, 2000); (vii) determination of the nucleation rate in undercooled liquids (De Panfilis & Filipponi, 2000), as described in the next section.

3. Measurements of the nucleation rate

In the analysis of the hysteresis curves obtained in the case of melting and undercooling, the levels of absorption corresponding to the solid and liquid phases show, in general, a linear variation with temperature. In the case of a sample that is only partly crystallized, the fraction of molten sample, $X_l(T)$, can be easily determined according to the level of absorption with respect to the extrapolations of the liquid and solid lines, as a function of temperature. This measurement together with information on the thermal history of the sample can be used to determine the nucleation rate, as described in detail in a recent publication (De Panfilis & Filipponi, 2000).

For a polydisperse sample with a known mass–droplet distribution, $\varphi(m)$, the fraction of molten sample as a function of time in the cooling process can be expressed as

$$X_l(t) = \frac{\int_0^\infty \mathrm{d}m\, m\, \varphi(m)\, \exp[-m\lambda(t)]}{\int_0^\infty \mathrm{d}m\, m\, \varphi(m)}, \qquad (3)$$

where $\lambda(t) = \int_0^t I[T(t')]\,\mathrm{d}t'$ depends on the integral of the nucleation rate over the thermal history. From the experimental $X_l(t)$ curve it is possible to obtain the function $\lambda(t)$ by numerical procedures. The nucleation rate $I(T)$ is obtained by time differentiation of the $\lambda(t)$ function and by reading this value as a function of the corresponding temperature, namely

$$I(T) = \left.\frac{\partial\lambda(t)}{\partial t}\right|_{t=t(T)}. \qquad (4)$$

This method, which is based uniquely on X-ray absorption measurements, allows one to measure $I(T)$ directly without any assumption on its functional form. This is at variance with other procedures based on single-event statistics and therefore this method warrants potential interest from the materials science community.

As described in §1, the nucleation rate is a fundamental physical property of undercooled liquids which represents the probability of rare fluctuations leading to crystallization. The picture provided by the classical theory of nucleation is certainly oversimplified and the availability of experimental data on $I(T)$ independent of any theoretical model may be very useful in order to understand and verify the validity of theoretical predictions.

4. Liquid structure determination by EXAFS

The previous techniques can be used to prepare a sample under controlled experimental conditions, possibly by monitoring *in situ* the transformation or decomposition of the precursor compound. In a second stage of the experiment, the sample can be melted and this process can be monitored by the temperature-scanning technique (Filipponi *et al.*, 1998). The observation of melting and of other phase transitions is extremely important because it allows one to check the correct measurement of the temperature and to reveal possible problems with the sample. The absence of a sharp melting point may indicate a spread of temperatures across the sample, the existence of impurities, or other artifacts. Because of the low sensitivity of XAFS to phase changes, XAFS cannot actually be used to guarantee that the new phase is actually reached after raising the presumed sample temperature above that of a phase transition. We therefore stress the importance of characterizing the sample phase with a suitable technique, such as that which we have developed. Once the sample has been prepared in the liquid (or undercooled liquid) state, high-quality X-ray absorption spectra can be collected using the normal scanning mode of the beamline.

The analysis of X-ray absorption spectra of samples in the liquid state is a complicated task because of the large disorder which characterizes the atomic distributions. Our group has made a substantial contribution in this field (Filipponi, 2001) based on a simple and effective procedure (Filipponi, 1994). For a liquid system, the structure is described in terms of the radial distribution function $g(r)$ or of a set of $n(n+1)/2$ partials for an n-component liquid, which usually present a broad and asymmetric first-neighbour peak followed by a weakly structured tail tending to 1 for $r \rightarrow \infty$. Apart from the case of molecular liquids, there is a continuous distribution of distances in a liquid and the $g(r)$ does not vanish after the first peak. For these reasons, a data analysis based on the fitting or determination of the shape of isolated peaks, such as that which is normally performed for solids, is bound to fail. Actually, the situation is even worse since a single shell peak can usually be fitted to liquid-phase data, but the results usually give inconsistent structures (Filipponi, 2001). The error lies in performing peak fitting with respect to a zero baseline corresponding to $g(r) = 0$. This is not appropriate for a liquid since it does not account for the long-range constraints that a structure should satisfy. In the procedure that we have proposed, the simplicity of the peak-fitting approach is retained, but the peaks are fitted on top of a non-zero baseline $g(r) = g_{\mathrm{tail}}(r)$, which, together with simple constraints in the peaks parameters,

accounts for the correct long-range behaviour of the fitted structure and related compressibility sum rules. The details of this approach are described elsewhere (Filipponi, 1994). This method has been widely applied by us and by other groups for the EXAFS determinations of liquid structures and the results were always found to be in excellent agreement with other structural determinations, when available for comparison. An extended reference list is reported for the convenience of the reader (Bowron *et al.*, 1998; D'Angelo & Pavel, 1999; D'Angelo *et al.*, 1994; Di Cicco, 1996; Di Cicco *et al.*, 1996, 1997, 1999, 2000; De Panfilis & Filipponi, 1997; Filipponi & Di Cicco, 1995; Filipponi *et al.*, 1997, 1999).

5. An example: undercooled liquid indium

An In sample composed of micrometre-scale powder dispersed in an inert *a*-B matrix was prepared starting from InP high-purity millimetre-size crystals. The InP crystals were crushed in a ball mill in the presence of ethyl alcohol. The resulting suspension was left for about 1 h to let the largest particles deposit. The finest particles were mixed with high-purity *a*-B powder and the dried mixture was pelleted to form a sample of thickness suitable for In *K*-edge measurements.

The sample InP/*a*-B pellet was inserted in the high-temperature oven (Filipponi & Di Cicco, 1994) and heated under high-vacuum conditions. The decomposition of InP into In (as a result of the volatilization of P) was monitored *in situ* using repeated scans at the In *K*-edge region. The evolution of these spectra is shown in Fig. 2. The InP decomposition occurs around 873 K. The sample was heated up to 1173 K and cooled to room temperature. The EXAFS spectra after the heat treatment (thick lines in Fig. 2) are clearly different from those of the original compound and indicate that an irreversible structural transformation has occurred.

Both chemical knowledge regarding the InP stability and regarding the absence of reactivity between In and B, together with the EXAFS evidence of Fig. 2, suggest that a complete reduction of InP into high-purity metallic In has occurred. This scenario is, however, only a conjecture until an unambiguous structural proof is obtained. With the present experimental setup (Filipponi, Borowski *et al.*, 2000; Filipponi, Di Cicco *et al.*, 2000), the proof can be obtained by performing an *in situ* energy-scanning X-ray diffraction measurement. In the present case of a sample of (supposedly) In powder in an *a*-B matrix, we have, for the first time, used the two-channel collimator system described above (§2.1). The corresponding powder diffraction pattern, collected at room temperature, is reproduced in Fig. 3. In Fig. 3, the powder pattern is compared, on the q scale, with a calculation for the In (body-centred) orthorhombic lattice with a = 3.253 and c = 4.9455 Å. The excellent agreement between calculated and measured positions and the perfect overlap between the three Bragg peaks recorded in both channels prove the success of the principle of operation of this multichannel detection ESXD system. For the specific application on the In/*a*-B sample, the diffraction check tells us that there are no other crystalline compounds in the sample besides In, that the original InP compound has been fully decomposed, and that no other crystalline compounds were formed in the sample treatment. The relatively high background should be associated with the diffuse scattering of *a*-B. The good reproduction of the intensity ratios between Bragg peaks indicates also that in this case excellent powder statistics were obtained, owing to the very small size of the final In particles. In the case of larger particles, the powder statistics are poor and intensity measurements are not reliable since they mainly reflect the fluctuations in the number of particles which happen to be in Bragg reflection. This is a drawback of working under high-resolution conditions, as can be appreciated by considering the narrow width of the Bragg peaks.

As a result of the large disorder in both the solid and the liquid phase, the In *K*-edge EXAFS is weak and very small differences can

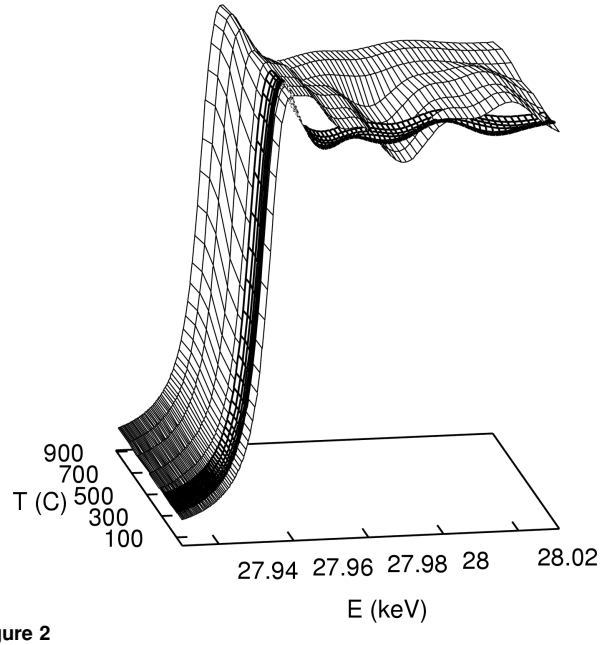

Figure 2
Indium *K*-edge spectra collected *in situ* during the decomposition of the InP powder into In liquid droplets. The thin lines represent the spectra collected while increasing T. The decomposition occurs mainly between the fifth and sixth spectrum around 873 K. The spectra obtained after quenching are reported as thick lines. They clearly differ from those of the initial sample.

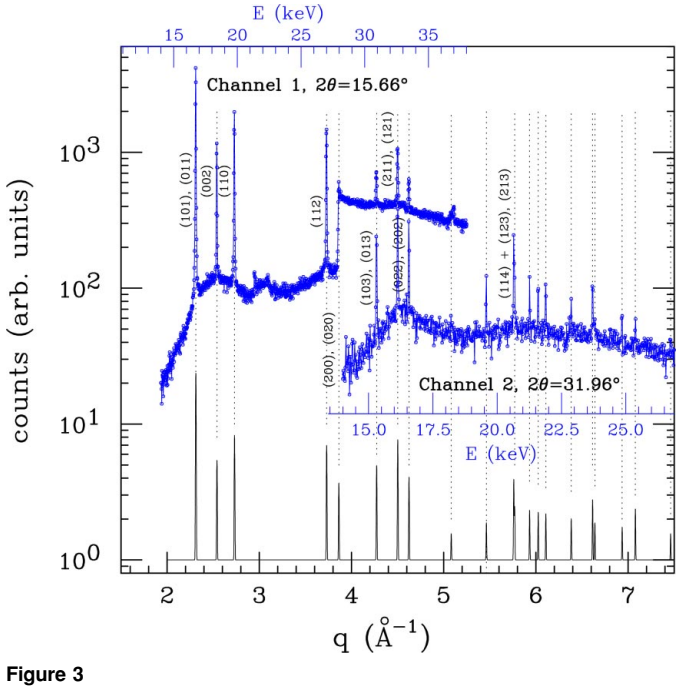

Figure 3
Example of the performance of the two-channel collimator detector for ESXD in the case of a sample of In powder in *a*-B matrix. The two spectra covering different q ranges have been collected simultaneously during the monochromator energy scan. The In powder diffraction pattern is clearly visible and overlap between several peaks in the two channels provides confidence regarding the validity of the technique. This result provides a confirmation of the correct sample preparation procedures.

be detected upon melting. In order to verify the correct melting behaviour expected for In and the undercooling capability of the micrometre-scale droplets in the *a*-B matrix, the sample was subjected to a temperature scan from 330 to 460 K, and back to 340 K, while measuring the absorption at E_1 = 28.000 and E_2 = 28.014 keV, corresponding (roughly) to the maximum and the minimum, respectively, of the first strong EXAFS oscillation. The measured $\Delta\alpha = \alpha(E_1) - \alpha(E_2)$ (amplitude of the EXAFS oscillation) as a function of T in the temperature scan is shown in Fig. 4. In the solid phase, $\Delta\alpha$ decreases with increasing T until it drops suddenly at T_m. This is direct evidence, from X-ray absorption, of the sample melting. The hysteresis shown by the $\Delta\alpha(T)$ experimental data provides clear evidence that the sample remains in an undercooled liquid state down to $T_u \simeq 355$ K in the cooling ramp. A rough estimate of the nucleation rate at $T_u \pm 10$ K can be obtained on the basis of the known time interval between data point (about 3.5 s) and the average In droplet size (~2 μm in diameter) resulting in a value of $I(T_u) \simeq 5 \times 10^{15}\ \mathrm{s^{-1}\ m^{-3}}$.

The undercooling range is $X_u = T_u/T_m \simeq 0.83$, which represents a very interesting value considering that, under these conditions, the sample can be subject to a complete structural investigation by EXAFS. High-quality In *K*-edge spectra were measured in the solid phase at 390 K, in the liquid at 500 K and in the undercooled liquid at 385 K. The corresponding $\chi(k)$ EXAFS spectra extracted using a standard polynomial spline are presented in Fig. 5 (solid at the top, liquid in the middle, undercooled liquid at the bottom) for comparison. The solid- and liquid-phase spectra differ considerably, as expected, in particular in the phase of the oscillation. The liquid and undercooled-liquid spectra are also slightly different, indicating that a change in the short-range structure can actually be probed by EXAFS.

All these preliminary results indicate that In is a quite interesting system for the application of a more detailed analysis of both the temperature scan of Fig. 4 and the EXAFS signal. Using the procedures described in §§3 and 4, we expect to improve the determination of $I(T)$ and to identify the actual structural changes occurring in the short-range shape of the $g(r)$.

6. Conclusion

In this paper, we have summarized and described our main achievements towards the realisation of an ideal setup for X-ray absorption spectroscopy investigations at high temperature and high pressure. The increasing complexity of XAFS experiments and the requirement for available *in situ* characterization techniques have stimulated us to enrich the standard experimental setups with additional experimental capabilities. We found that it is possible to add to any energy-scanning EXAFS facility a system based on fixed-angle collimator detectors for the collection of powder X-ray diffraction patterns. A multichannel detector system can also be employed for a more efficient usage of the beam time; the validity of its principle of operation has been demonstrated in this paper. An additional very useful experimental tool was found to be the possibility to perform controlled temperature scans on the sample. With this technique, it is possible to monitor and to determine several important physical quantities connected with phase transitions. The scientific research program, aimed at investigating the structure and nucleation rate in the undercooled state of liquid matter, has largely benefited from the development of these novel experimental techniques. In particular, the reliability of the experimental results under these challenging and elusive conditions largely improved. An example of how these techniques can be used to produce and characterize a sample of In suitable for performing physical measurements in the undercooled liquid state has been presented.

All these procedures are applicable to a wide class of experiments under extreme conditions of high temperature and pressure, but also

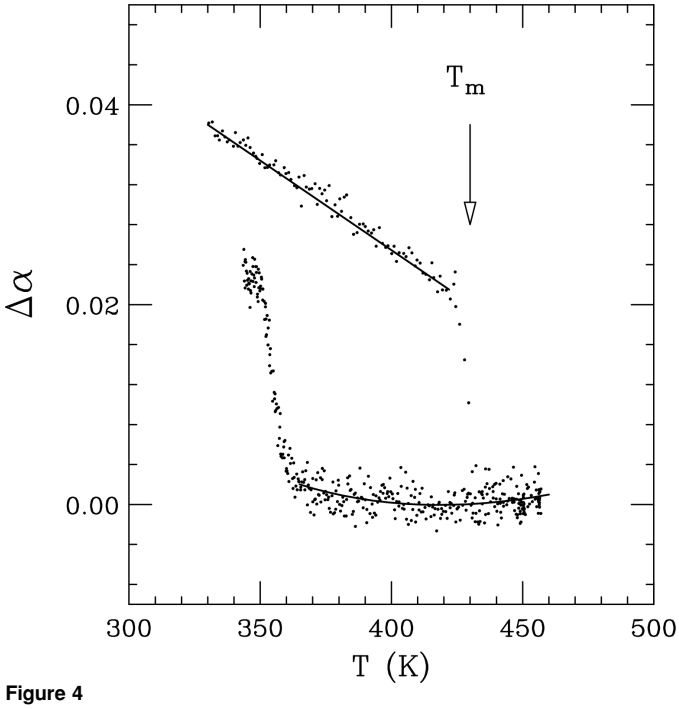

Figure 4
X-ray absorption temperature scan illustrating the melting (at T_m) and undercooling of the In powder sample. The absorption difference $\Delta\alpha = \alpha(E_1) - \alpha(E_2)$ (between E_1 = 28.000 and E_2 = 28.014 keV) roughly corresponds to the amplitude of the main EXAFS oscillation of the In *K*-edge spectrum.

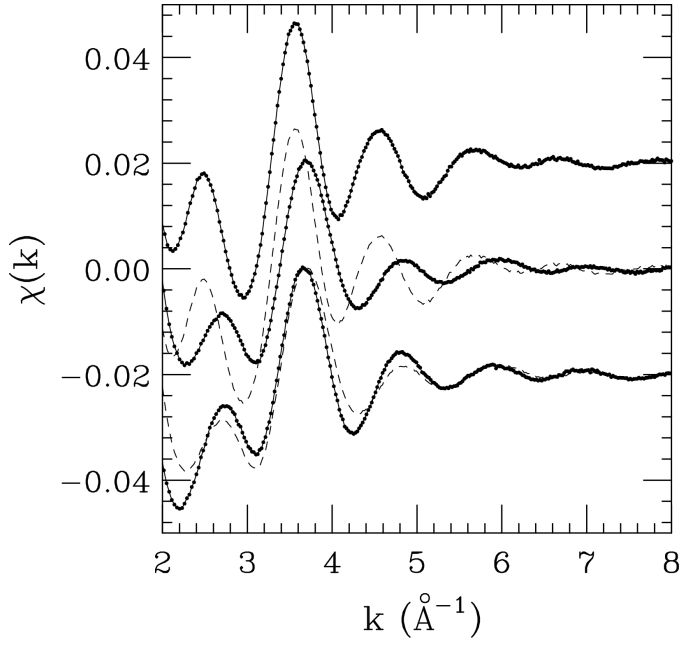

Figure 5
Comparison of the EXAFS spectra of solid In at 390 K (top and dashed line in the middle), in the liquid at 500 K (middle and bottom dashed line) and in the undercooled liquid at 385 K (bottom). The differences indicate the existence of short-range structural changes, not only between the solid and liquid but also in the liquid phase upon undercooling.

we believe that they may prove useful for experiments under standard conditions. In conclusion, we suggest that several other facilities may benefit from the application and further development of these ideas.

Most of the results presented in this paper have been obtained within the framework of the HS1197 ESRF long-term project. We are greatly indebted to the ESRF staff for technical assistance during and prior to the experiments.

References

Besson, J. M., Nelmes, R. J., Hamel, G., Loveday, J. S., Weill, G. & Hull, S. (1992). *Physica B*, **180/181**, 907–910.

Bowron, D. T., Filipponi, A., Lobban, C. & Finney, J. L. (1998). *Chem. Phys. Lett.* **293**, 33–37.

Buontempo, U., Filipponi, A., Martínez-García, D., Postorino, P., Mezouar, M. & Itiè, J. P. (1998). *Phys. Rev. Lett.* **80**, 1912–1915.

Buontempo, U., Filipponi, A., Postorino, P. & Zaccari, R. (1998). *J. Chem. Phys.* **108**, 4131–4137.

Clausen, B. S. (1998). *Catal. Today*, **39**, 293–300.

D'Angelo, P., Nola, A. D., Filipponi, A., Pavel, N. V. & Roccatano, D. (1994). *J. Chem. Phys.* **100**, 985–994.

D'Angelo, P. & Pavel, N. V. (1999). *J. Chem. Phys.* **111**, 5107–5115.

Dent, A. J., Wells, M. P., Farrow, R. C., Ramsdale, C. A., Derbyshire, G. E., Greaves, G. N., Couves, J. W. & Thomas, J. M. (1992). *Rev. Sci. Instrum.* **63**, 903–906.

De Panfilis, S. & Filipponi, A. (1997). *Europhys. Lett.* **37**, 397–402.

De Panfilis, S. & Filipponi, A. (2000). *J. Appl. Phys.* **88**, 562–570.

Di Cicco, A. (1996). *Phys. Rev. B*, **53**, 6174–6185.

Di Cicco, A. (1998). *Phys. Rev. Lett.* **81**, 2942–2945.

Di Cicco, A., Aquilanti, G., Minicucci, M., Filipponi, A. & Rybicki, J. (1999). *J. Phys. Condens. Matter*, **11**, L43–L49.

Di Cicco, A., Minicucci, M. & Filipponi, A. (1997). *Phys. Rev. Lett.* **78**, 460–463.

Di Cicco, A., Rosolen, M. J., Marassi, R., Tossici, R., Filipponi, A. & Rybicki, J. (1996). *J. Phys. Condens. Matter*, **8**, 10779–10797.

Di Cicco, A., Taglienti, M., Minicucci, M. & Filipponi, A. (2000). *Phys. Rev. B*, **62**, 12001–12013.

Filipponi, A. (1994). *J. Phys. Condens. Matter* **6**, 8415–8427.

Filipponi, A. (1996). *J. Phys. Condens. Matter*, **8**, 9335–9339.

Filipponi, A. (2001). *J. Phys. Condens. Matter.* In the press.

Filipponi, A., Borowski, M., Bowron, D. T., Ansell, S., De Panfilis, S., Di Cicco, A. & Itiè, J.-P. (2000). *Rev. Sci. Instrum.* **71**, 2422–2432.

Filipponi, A., Borowski, M., Loeffen, P. W., De Panfilis, S., Di Cicco, A., Sperandini, F., Minicucci, M. & Giorgetti, M. (1998). *J. Phys. Condens. Matter*, **10**, 235–253.

Filipponi, A., Bowron, D. T., Lobban, C. & Finney, J. L. (1997). *Phys. Rev. Lett.* **79**, 1293–1296.

Filipponi, A. & Di Cicco, A. (1994). *Nucl. Instrum. Methods Phys. Res. B*, **93**, 302–310.

Filipponi, A. & Di Cicco, A. (1995). *Phys. Rev. B*, **51**, 12322–12336.

Filipponi, A., Di Cicco, A., Aquilanti, G., Minicucci, M., De Panfilis, S. & Rybicki, J. (1999). *J. Non-Cryst. Solids*, **250–252**, 172–176.

Filipponi, A., Di Cicco, A. & De Panfilis, S. (1999). *Phys. Rev. Lett.* **83**, 560–563.

Filipponi, A., Di Cicco, A. & De Panfilis, S. (2000). *Phys. Status Solidi B*, **219**, 267–277.

Hosokawa, S., Tamura, K., Inui, M., Yao, M., Endo, H. & Hoshino, H. (1992). *J. Chem. Phys.* **97**, 786–791.

Jacobs, G. & Egry, I. (1999). *Phys. Rev. B*, **59**, 3961–3968.

Jacobs, G., Egry, I., Maier, K., Platzek, D., Reske, J. & Frahm, R. (1996). *Rev. Sci. Instrum.* **67**, 3683–3687.

Katayama, Y., Mezouar, M., Itié, J. P., Besson, J. M., Syfosse, G., Le Fevre, P. & Di Cicco, A. (1997). *J. Phys. IV*, **7**(C2), 1011–1012.

Katayama, Y., Shimomura, O. & Tsuji, K. (1999). *J. Non-Cryst. Solids*, **250–252**, 537–541.

Ottaviano, L., Filipponi, A. & Di Cicco, A. (1994). *Phys. Rev. B*, **49**, 11749–11758.

Sankar, G., Wright, P. A., Natarajan, S., Thomas, J. M., Greaves, G. N., Dent, A. J., Dobson, B. R., Ramsdale, C. A. & Jones, R. H. (1993). *J. Phys. Chem.* **97**, 9550–9554.

Tamura, K., Inui, M. & Hosokawa, S. (1995). *Rev. Sci. Instrum.* **66**, 1382–1384.

Turnbull, D. (1950). *J. Appl. Phys.* **21**, 1022–1028.

Wallen, S. L., Palmer, B. J. & Fulton, J. L. (1998). *J. Chem. Phys.* **108**, 4039–4046.